SUPPLEMENTARY DATA

Sequence of Protein Kinase actions to create the primary Slimb binding site in Ci.

To investigate which protein kinases phosphorylated S852 and surrounding residues we used an antibody raised against a Ci peptide centered on phosphorylated S852 (CGSMQSpRRSSQS). This antibody recognized GST-Ci on Western blots after phosphorylation by both PKA and GSK3, as expected, but additional phosphorylation with CK1 prevented antibody recognition (Figure S2A). We suspected that the phosphorylated S852 epitope was no longer recognized if S855 was also phosphorylated (by CK1 primed by pS852). We therefore used GST-Ci-S855A ("S_{852}RR**A**S") to measure S852 phosphorylation in the absence of confounding effects related to S855 phosphorylation. Phosphorylated S852 was detected in the S_{852}RR**A**S variant following phosphorylation by PKA and GSK3 together, by all three kinases together or by just PKA and CK1 together (Figure S2A), implying that S852 can be phosphorylated by CK1 following initial priming by PKA site 1 (Figure S2E). As expected, Ala substitution at PKA site 1 ("P1A") in the S_{852}RR**A**S variant eliminated phosphorylation of S852 in response to PKA and CK1 (Figure S2A). Similarly, CK1 phosphorylation of S852 was drastically reduced by substitution of S849 with Ala (Figure S2B), implying that phosphorylated S849 primes CK1 phosphorylation of S852. Alteration of T845 produced only a small reduction in S852 phosphorylation by CK1 (Figure S2B), suggesting that phosphorylated S844 can prime CK1 phosphorylation of S849 in the absence of phosphorylated T845.

We have shown that S849 phosphorylation is essential for Slimb binding and occurs robustly in the presence of CK1 following phosphorylation of PKA site 1. Accordingly, Ala substitution at PKA site 1 eliminates Slimb binding stimulated by just PKA and CK1 (Figure S2C). However, this variant ("P1A") still binds Slimb quite well if GSK3 is also included. To

account for this observation we suggest an additional path for creating the Slimb binding motif; PKA site 2 primes phosphorylation of S852 by GSK3, which then primes GSK3 phosphorylation of a non-consensus site (S849), followed by T845 and S841 (Figure S2F). Phosphorylated S841 would then prime S844 phosphorylation by CK1. Consistent with this proposal, we found that Slimb binding of P1A was stimulated much more efficiently by treatment with PKA and GSK3 followed by CK1 than by treatment with PKA and CK1 followed by GSK3 (Figure S2D). It is likely that S849 is phosphorylated much more efficiently by CK1 (Figure S2E) than by GSK3 (Figure S2F) in vitro and in vivo because GSK3 phosphorylates such non-consensus substrates very inefficiently (Ilouz et al., 2006; Kobe et al., 2005).

Fly crosses

In all, female genotype is first:

yw hs-flp ; ubi-GFP FRT40A / Cyo ; C765 hh-lacZ / TM6B or *yw hs-flp ; ubi-GFP FRT40A cl2L3/ Cyo ; C765 ptc-lacZ / TM6B* were crossed to *yw ; smo^{2} FRT40A / CyO; UAS-Ci* to generate *smo* mutant clones or *yw ; smo^{2} $pka\text{-}c1^{B3}$ FRT40A / CyO ; UAS-Ci* to generate *smo pka* mutant clones.

yw hs-flp UAS-GFP; tub-Gal80 FRT40A /CyO; C765 hh-lacZ/TM6B were crossed to *yw; FRT40A/CyO; UAS-Ci* to generate clones lacking *tub-Gal80* and hence expressing *UAS-GFP* and *UAS-Ci* via *C765-GAL4*.

yw hs-flp ; smo^{2} FRT42B P[smo^{+}] ubi-GFP ; C765 ptc-lacZ/TM6B were crossed to *yw; smo^{2} FRT42B $cos2^{W1}$/CyO; UAS-Ci* to generate *smo cos2* double mutant clones.

yw hs-flp fu^{mH63} ; FRT42B P[y^{+}] P[fu+]/CyO ; C765 ptc-lacZ/TM6B were crossed to *yw ; UAS-Ci* to generate *y* males mutant for *fu.*

yw hs-flp ; hs-CD2 FRT39 ptc-lacZ/CyO ; FRT82B ubi-GFP/TM6B were crossed to *yw ; FRT82B $slimb^{1}$/TM6B* to generate *slimb* mutant clones.

yw hs-flp; ubi-GFP FRT40A/CyO ; C765 ptc-lacZ/TM6B were crossed to *yw; pka-C1^{H2} FRT40A to* generate *pka* clones.

yw hs-flp ; pka-C1^{E95} FRT39/CyO ; FRT82B ubi-GFP/TM6B were crossed to *yw ; hs-CD2 FRT39A ptc-lacZ/CyO ; FRT82B slimb^{1}/TM6B* to generate discs with *pka* and *slimb* mutant clones.

yw hs-flp ; FRT42B ubi-GFP/CyO; C765 ptc-lacZ/TM6B were crossed to *yw ; FRT42B cos2^{W1}/CyO* or *yw; FRT42B cos2^{W1}/CyO ; UAS-Ci* to generate *cos2* clones.

yw hs-flp ; pka-C1^{H2} FRT42B [pka-C1^{+}] ubi-GFP/CyO ; C765 ptc-lacZ / TM6B were crossed to *yw*; *pka-C1^{H2} FRT42B cos2^{W1}/CyO* to generate *cos2 pka* double mutant clones.

yw hs-flp ; ubi-GFP FRT40A cl2L3/CyO; C765 hh-lacZ/TM6B were crossed to *yw; smo^{2} nedd8^{AN015} FRT40A/CyO; UAS-Ci* to generate *smo nedd8* clones.

yw hs-flp; ubi-GFP FRT40A cl2L3/CyO; C765 ptc-lacZ/TM6B were crossed to *yw; nedd8^{AN015} FRT40A/CyO* to generate *nedd8* mutant clones.

Supplementary Figure Legends

Figure S1. Processing of variants of Ci-155 to Ci-75 in vivo.

(A-F) *smo* mutant clones (arrowheads) lacking GFP (green) were generated in wing discs expressing the indicated transgenes at 29C under the control of *C765-Gal4*. *hh-lacZ* expression (red) in posterior cells (right) was repressed in *smo* mutant clones by Ci-WT (A), Ci-Ds2 (C), Ci-G3A [S888A] (D), Ci-Us3 (E) and Ci-SRRAS [S855A/S891A] (F), but not by Ci-S849A (B), indicating that only Ci-S849A cannot be processed to Ci-75.

Figure S2. Phosphorylation cascades that create the primary Slimb binding site in Ci.

(A) Western blots of phosphorylated GST-Ci (WT; SRRSS) and variants with Ala substitution of S855 (black dot in E, F) alone (SRRAS) or together with Ala substitution of PKA site 1 (P1A+SRRAS) using antibody raised against a peptide centered on phosphorylated G2 (S852; green in E, F). The antibody only recognizes phosphorylated S852 if S855 is not phosphorylated by CK1, so S852 phosphorylation is best assayed in GST-Ci proteins with an S855A ("SRRAS") substitution. In the SRRAS variant phosphorylation of S852 by CK1, primed initially by PKA site 1, is detected but S852 phosphorylation by GSK3 is more efficient. (B) Western blots of phosphorylated SRRAS and variants with T845A, S849A and Y846G substitutions using antibody to phosphorylated S852. The efficiency of PKA-primed GSK3 phosphorylation is similar in each case but PKA-primed CK1 phosphorylation of S852 is greatly reduced by the S849A substitution and slightly reduced in the T845A variant. The Y846G substitution does not increase the efficiency of S852 phosphorylation by CK1. (C, D) Flag/HA-Slimb-Myc binding to GST-Ci variants (as in Figure 1) showing (C) no response to PKA plus CK1 in the absence of PKA site 1 (P1A; S838A) and (D) that phosphorylation of GST-Ci-P1A first ("1") with PKA and GSK3, before CK1 ("2") stimulates Slimb binding better than PKA and CK1 ("1"), followed by GSK3 ("2"). (E, F) Residues between PKA sites 1 and 2 (P1, P2; red) that contribute to Slimb binding (underlined) can be phosphorylated (E) by CK1 alone (blue arrows) after initial priming by P1 (and S852 phosphorylation can be supplemented by GSK3 primed by P2 (green arrow)), or (F) less efficiently by consecutive GSK3 phosphorylation primed initially by P2 (green arrows) followed by CK1 (blue arrow). Phosphorylation motifs deviating from the most favored consensus are shown by dotted horizontal arrows.

Figure S3. Loss of *sgg* or *nedd8* does not completely block Ci-155 processing to Ci-75 repressor; Ci-U is not significantly processed to Ci-75.

(A-C) Repression of *hh-lacZ* expression (red) in mutant clones marked by the loss of GFP (green) was assayed for (A) *smo sgg* double mutant clones in discs expressing Ci-WT, (B) *smo* mutant clones in discs expressing Ci-U and (C) *smo nedd8* mutant clones in discs expressing Ci-WT. Processing of wild-type Ci-155 to Ci-75 is readily detected in *smo* clones lacking *sgg* or *nedd8* activity but Ci-U is not substantially processed to Ci-75. (D) Full-length Ci-WT-Myc levels (red) were increased in anterior *nedd8* mutant clones (arrowheads) marked by the loss of GFP (green). In each case *ci* transgenes were expressed using *C765-GAL4* at 29C.

Figure S4. Binding between Slimb and GST-Ci variants.

(A) Ci-SRRAS (S855A/S891A) and Ci-Ds2 (S858A/S859A/S862A/S863A) were assayed as GST-Ci proteins for Slimb binding as in Figure 1. (B) GST-Ci variants with the listed sequence alterations in the region preceding PKA site 3 were assayed for Slimb binding as in Figure 1. Neither promoting S878 phosphorylation by converting it to a PKA site (RRAS[red] to form "SpFYDPISp") nor substituting the Gli-2/3 sequence, DSYDPIS and ensuring CK1 phosphorylation of the first Ser in this motif (blue) by creating a PKA priming site (RRST[red]; to form "DSpYDPISp") increased GST-Ci binding to Slimb or allowed binding in response to just PKA and GSK3 (not shown). Substitution of the SFYDPIS motif of Ci with a β-TRCP binding site consensus sequence from β-catenin that is phosphorylated by GSK3 primed initially by PKA site 3 (to form "DSpGIHSp") increased Slimb binding relative to GST-Ci-WT phosphorylated by PKA, CK1 and GSK3.

Figure S5. GST-Ci binds to higher order SCF complexes.

(A) Binding of GST-Ci to Slimb and SkpA in extracts of cells co-transfected with Flag/HA-Slimb-Myc and Flag/HA-SkpA-Myc expression vectors. Bound proteins probed with HA antibody show a similar dependence on GST-Ci phosphorylation. (B) Binding of GST-Ci and GST-Ci-SL to endogenous Cul1 in extracts containing Flag/HA-Slimb-Myc probed with antibody to Cul1. Neddylated Cul1 (Cul1-N8) is inferred from the characteristically shifted band. Relative binding of each Cul1 form is shown numerically. (C) In addition to R333A and R353A we altered two residues (R374E and S391E) homologous to those in β-TRCP that interact directly with pS37 in β-catenin (Wu et al., 2003) to create Slimb-NB. Binding of Flag/HA-Slimb-NB (R333A/R353A/R374E/S391E) expressed alone or with Myc-Slimb to GST-Ci, detected by Flag antibody. Myc-WT allows some binding of Slimb-NB to phosphorylated GST-Ci, presumably by binding to both GST-Ci and Slimb-NB.

Figure S6. Effect of *pka*, *slimb* and *pka slimb* mutant clones on the Hh target genes, *ptc* and *en*.

(A-J) *pka* (A-E) and *slimb* (F-J) mutant clones marked by the absence of GFP (green in A, D-F, I, J) were generated in wing discs to analyze expression of *ptc-lacZ* (*plz*; blue in B, D, G, I) and En (red in C, E, H, J) in the anterior compartment where endogenous Ci is expressed. There is clear ectopic expression of *ptc-lacZ* and En in *pka* mutant clones (B, C) but not in *slimb* mutant clones (G, H). (K-T) Two examples of wing discs carrying three clonal genotypes: *pka* mutant clones marked by the absence of CD2 (blue in K, L, P, Q), *slimb* mutant clones marked by the absence of GFP (green in M, N, R, S), and *pka slimb* double mutant clones marked by the absence of both GFP and CD2. Within the wing pouch, there is ectopic expression of *ptc-lacZ* in *pka* (yellow arrowhead in K-O) and *slimb pka* mutant clones (arrows in K-O and P-T) but not in *slimb* clones (white arrowheads in K-O and P-T). The disc in (P-T) also shows a *slimb* mutant clone outside of the wing pouch (yellow arrowhead),

which produces some ectopic *ptc-lacZ* expression. Induction of *ptc-lacZ* in *slimb* mutant clones was seen only outside the wing pouch and only in discs that were also heterozygous for *PKA-C1*.

Figure S7. PKA-dependent proteolysis of Ci-U but not Ci-S849A.

(A-L) Full-length Ci protein levels resulting from expression of *UAS-Flag/HA-Ci-Myc* transgenes using *C765-GAL4* at 29C were assayed by staining for the C-terminal Myc epitope (red). (A-I) Stabilization of full-length protein by Hh was seen for Ci-WT and Ci-U, but not Ci-S849A by higher Myc staining in posterior (right) than anterior cells of wild-type (A-C) and fu^{mH63} mutant (D-F) wing discs, and by reduced Myc staining (red) in posterior *smo* mutant clones (arrowheads, G-I), marked by loss of GFP (green). (J-L) Increased Myc staining (red) of Ci-WT (J) and Ci-U (K) but not Ci-S849A (L) in anterior *smo PKA* mutant clones (arrowheads), marked by loss of GFP (green) indicates PKA-dependent proteolysis.

Figure S8. Cos2 does not significantly restrict Ci activity in the absence of PKA-dependent proteolysis.

(A-C) *pka* (A), *cos2* (B), and *pka cos2* (C) mutant clones were generated in wing discs and marked by the absence of GFP (green). Discs were stained with Engrailed antibody (red) to detect ectopic expression in mutant clones in the anterior compartment where Ci is endogenously expressed (A', B', C'). Merged images are shown (A", B", C"). Induction of En is stronger in *pka* than *cos2* mutant clones and is not increased further in *pka cos2* double mutant clones.

Figure S9. Cos2 is required for Hh-dependent activation of Ci.

(A, B) *cos2* clones (marked by the absence of GFP) were generated in discs expressing Ci-S849A at 20C (A) or Ci-WT at 29C and stained with antibody for *ptc-lacZ* expression (red). Arrows mark

posterior clones, showing a significant reduction in *ptc-lacZ* expression in mutant clones expressing Ci-S849A at 20C (A) but no significant reduction when Ci-WT is expressed at higher levels by incubation at 29C (B).

Figure S1

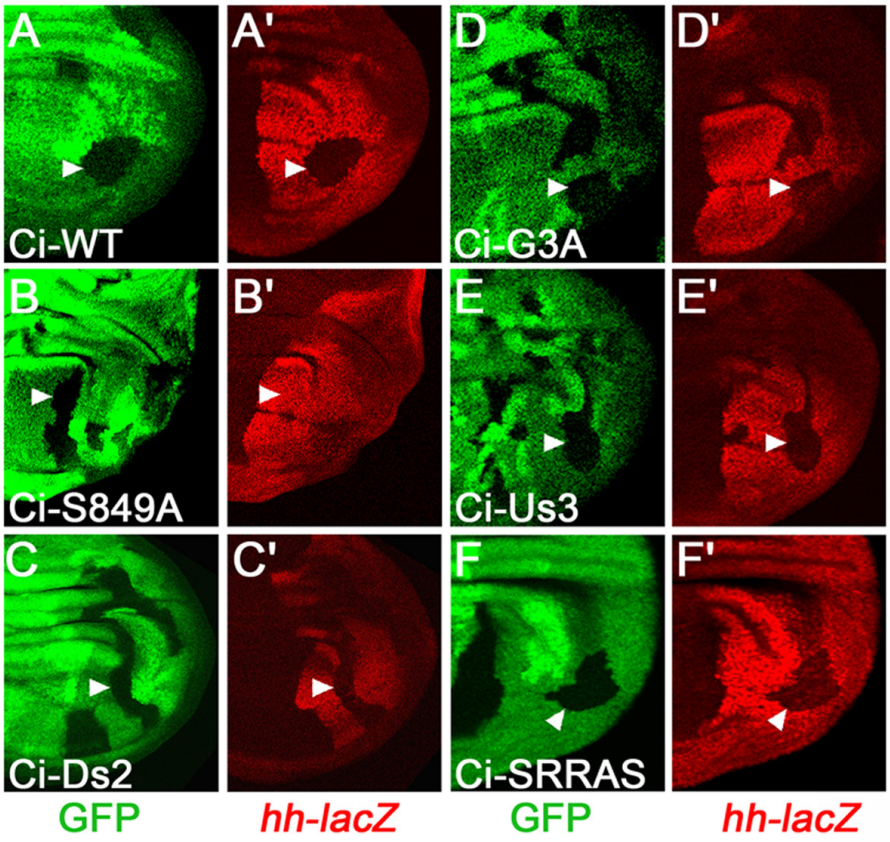

Figure S1

Figure S2

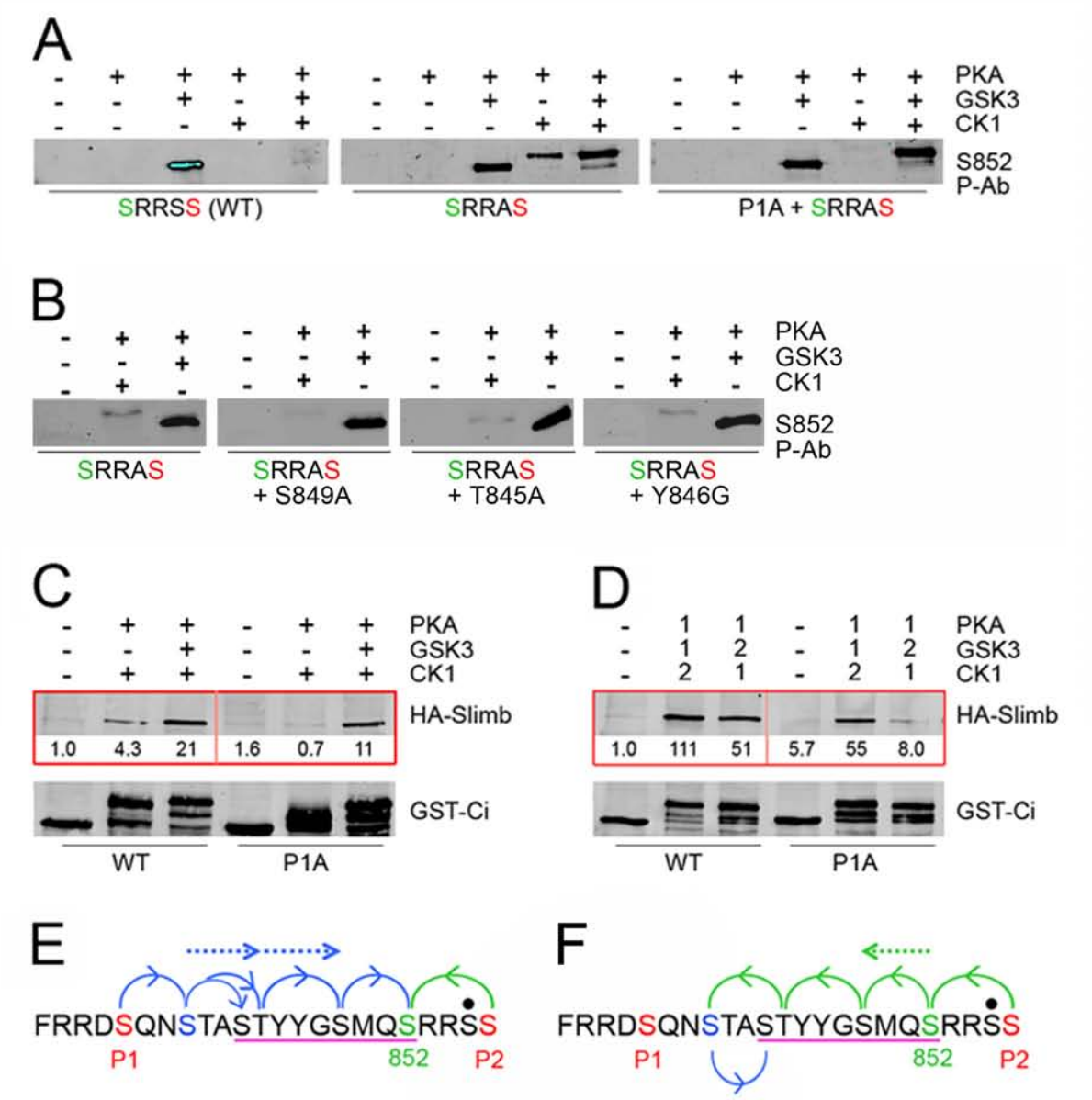

Figure S2

Figure S3

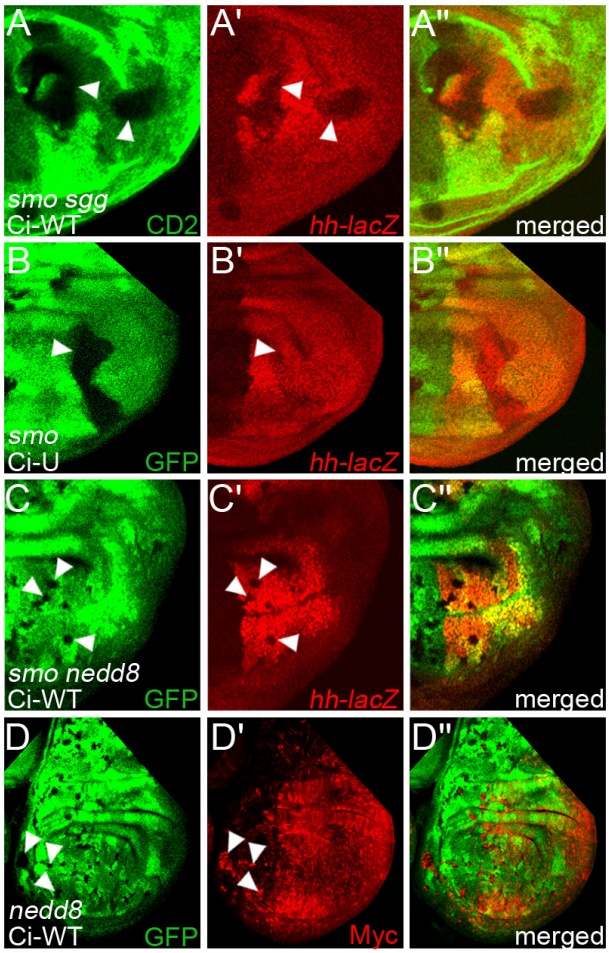

Figure S3

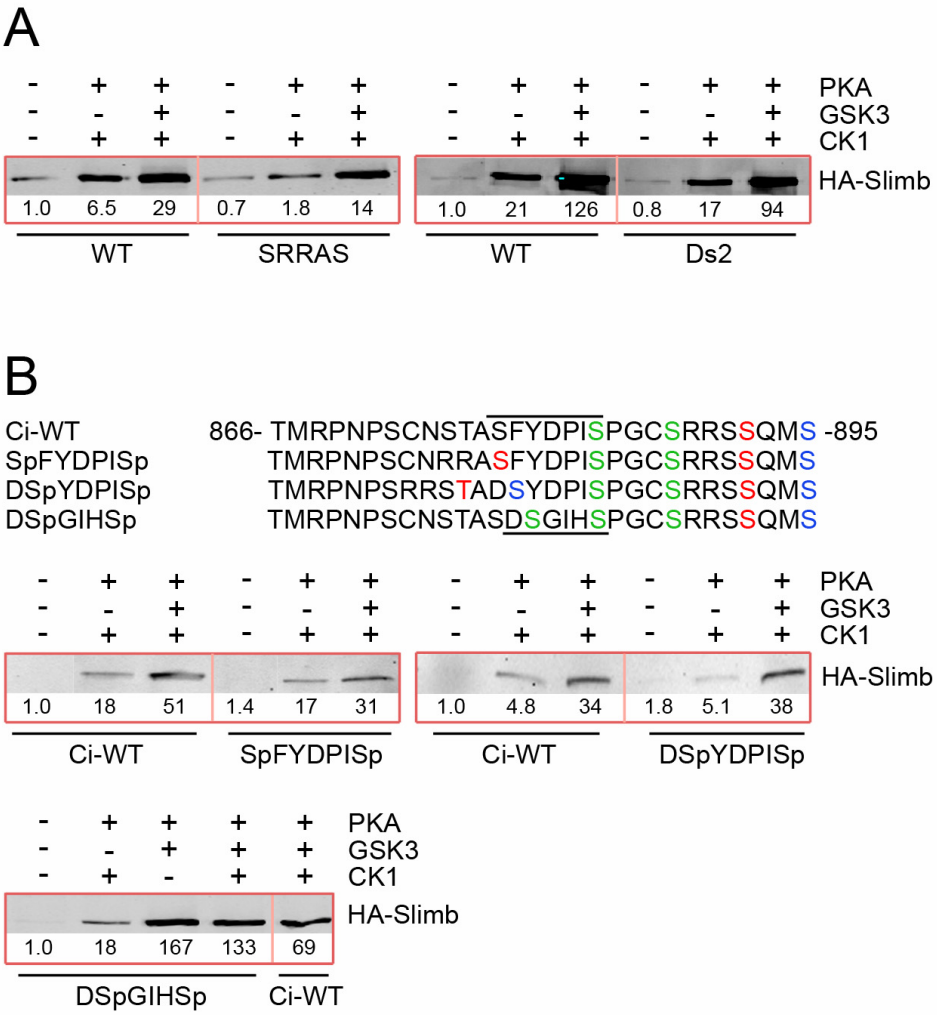
A
PKA
GSK3
CK1
HA-Slimb
1.0 6.5 29 0.7 1.8 14 1.0 21 126 0.8 17 94
WT SRRAS WT Ds2
B
Ci-WT 866- TMRPNPSCNSTASFYDPISPGCSRRSSQMS -895
SpFYDPISp TMRPNPSCNRRASFYDPISPGCSRRSSQMS
DSpYDPISp TMRPNPSRRSTADSYDPISPGCSRRSSQMS
DSpGIHSp TMRPNPSCNSTASDSGIHSPGCSRRSSQMS
PKA
GSK3
CK1
HA-Slimb
1.0 18 51 1.4 17 31 1.0 4.8 34 1.8 5.1 38
Ci-WT SpFYDPISp Ci-WT DSpYDPISp
PKA
GSK3
CK1
HA-Slimb
1.0 18 167 133 69
DSpGIHSp Ci-WT

Figure S4

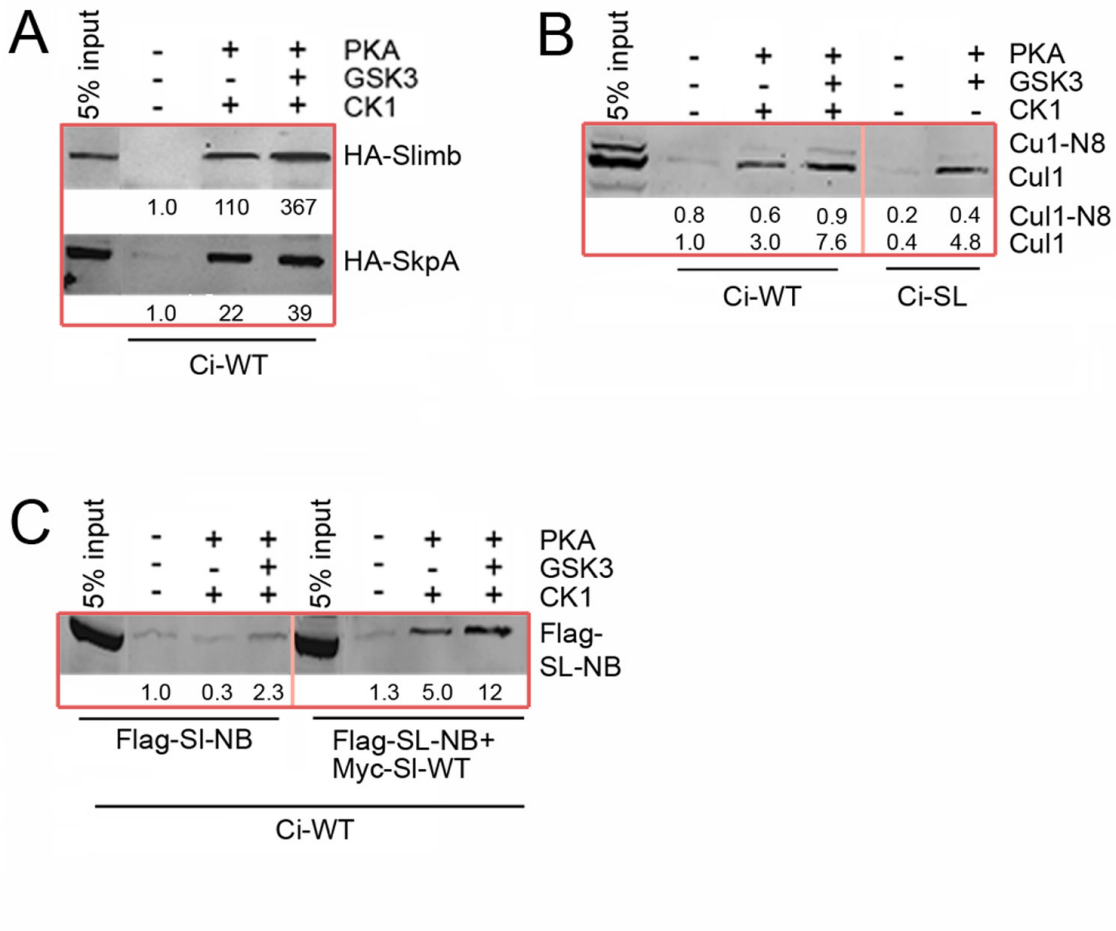
A
5% input
PKA
GSK3
CK1
HA-Slimb
1.0 110 367
HA-SkpA
1.0 22 39
Ci-WT
B
5% input
PKA
GSK3
CK1
Cu1-N8
Cul1
0.8 0.6 0.9 0.2 0.4
1.0 3.0 7.6 0.4 4.8
Cul1-N8
Cul1
Ci-WT
Ci-SL
C
5% input
5% input
PKA
GSK3
CK1
Flag-SL-NB
1.0 0.3 2.3 1.3 5.0 12
Flag-Sl-NB
Flag-SL-NB+
Myc-Sl-WT
Ci-WT

Figure S5

Figure S6

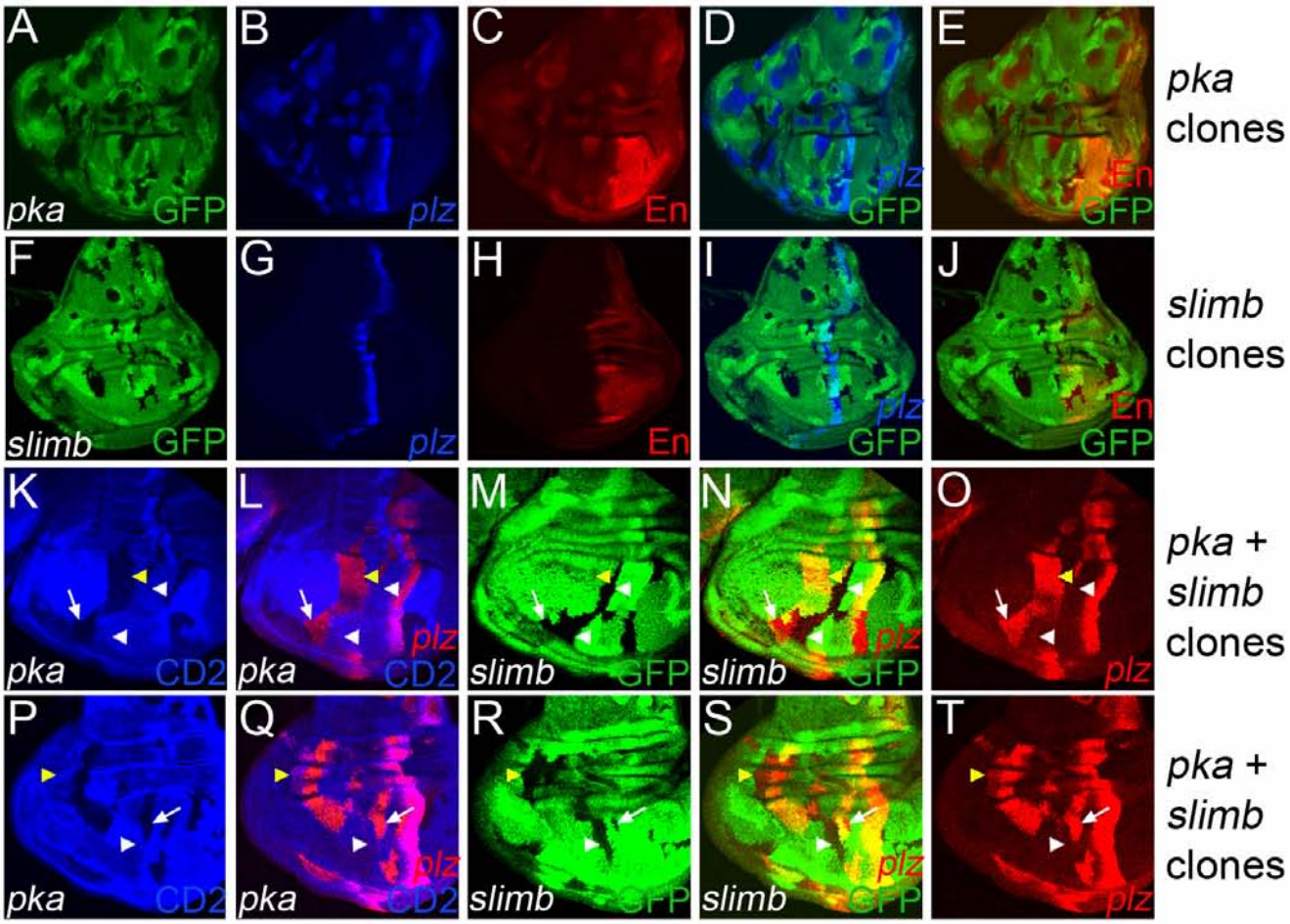

Figure S6

Figure S7

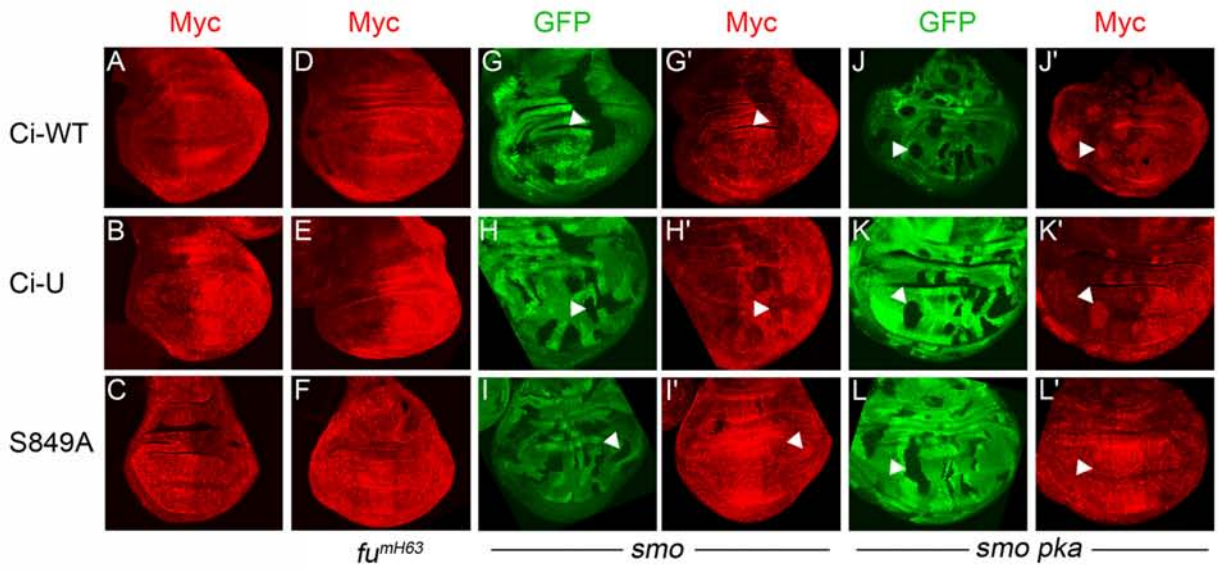

Figure S7

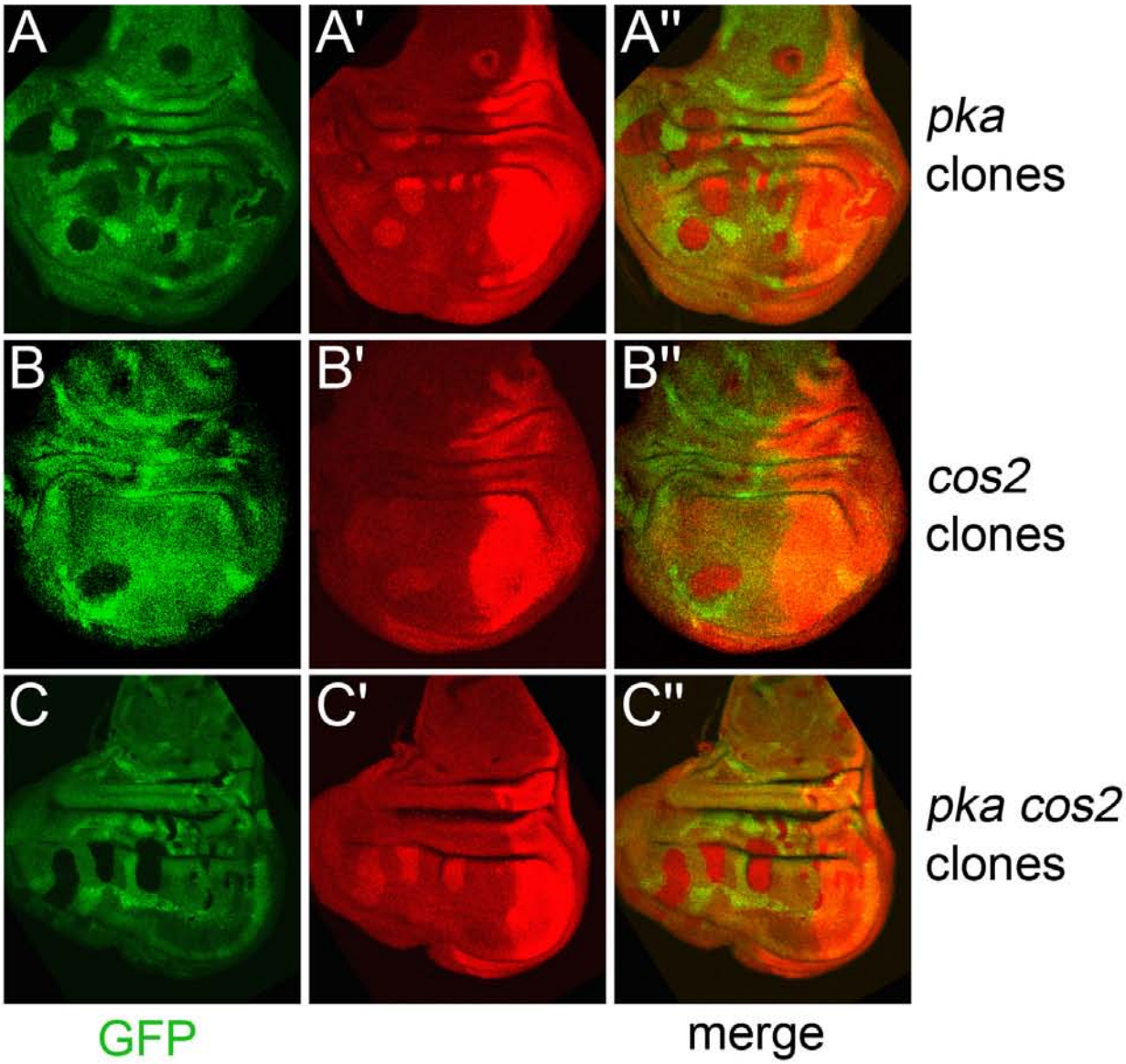

Figure S8

Figure S9

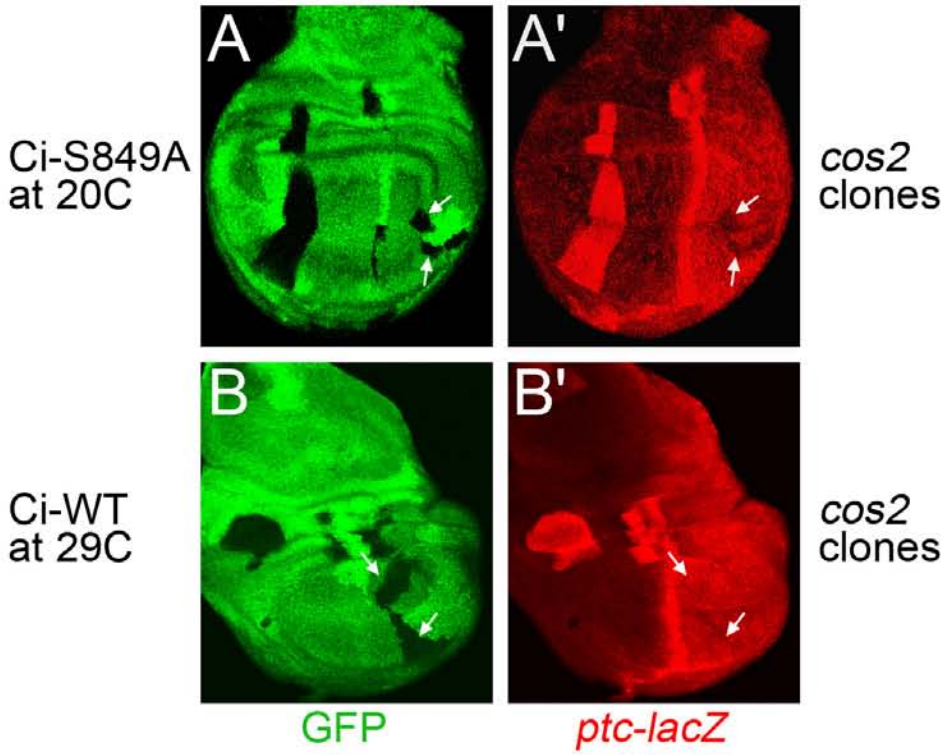

Figure S9